N79-20039

D9

9

AN EVALUATION OF FOUR SINGLE ELEMENT AIRFOIL ANALYTIC METHODS*

R. J. Freuler and G. M. Gregorek
General Aviation Airfoil Design and Analysis Center
The Ohio State University

SUMMARY

A comparison of four computer codes for the analysis of two-dimensional single element airfoil sections is presented for three classes of section geometries. Two of the computer codes utilize vortex singularities methods to obtain the potential flow solution. The other two codes solve the full inviscid potential flow equation using finite differencing techniques, allowing results to be obtained for transonic flow about an airfoil including weak shocks. Each program incorporates boundary layer routines for computing the boundary layer displacement thickness and boundary layer effects on aerodynamic coefficients.

Computational results are given for a symmetrical section represented by an NACA 0012 profile, a conventional section illustrated by an NACA 65A413 profile, and a supercritical type section for General Aviation applications typified by a NASA LS(1)-0413 section. Experimental results from The Ohio State University 15 cm (6 in.) by 56 cm (22 in.) Transonic Airfoil Tunnel are also given. The cases presented include operating conditions at subsonic, subcritical, and near critical or supercritical Mach numbers. The four codes are compared and contrasted in the areas of method of approach, range of applicability, agreement among each other and with experiment, individual advantages and disadvantages, computer run times and memory requirements, and operational idiosyncrasies.

INTRODUCTION

The General Aviation Airfoil Design and Analysis Center (GA/ADAC) was established at The Aeronautical and Astronautical Research Laboratory (AARL), The Ohio State University, under contract to NASA Langley Research Center in June 1976. GA/ADAC offers a comprehensive service to the general aviation community in the form of airfoil selection and design and analysis work as well as consultation in the areas of wind tunnel testing and flight testing work. An important feature of GA/ADAC is the large library of computer codes which has been established and is maintained at AARL. This computer program library re-

*This work has been supported in part by NASA Langley Research Center Contract NAS1-14406.

INTENTIONALLY BLANK

presents a wide variety of airfoil related computer codes collected in one location onto one computer system, with more than thirty computer codes in the areas of single element airfoil analysis and design, multi-element airfoil analysis and design, wing analysis, and propeller aerodynamic and acoustic performance analysis available for use.

A comparative evaluation of the four computer codes most frequently used at GA/ADAC for the analysis of two-dimensional single element airfoil sections is presented in this paper for three classes of airfoil section geometries: symmetric, conventionally cambered, and aft-cambered. Theoretical predictions of pressure distributions and aerodynamic coefficients for the three airfoils are compared with measurements taken in the 15 cm x 56 cm Transonic Airfoil Tunnel at AARL.

The symbols used herein are defined in an appendix.

COMPUTER CODES

The computer codes used for the comparisons are designated as follows: (1) Garabedian, by F. Bauer, P. Garabedian, D. Korn, and A. Jameson and detailed in references 1 and 2; (2) Carlson, by L. A. Carlson and explained in references 3 and 4; (3) Smetana, by F. Smetana, D. Summey, N. Smith, and R. Carden and documented in references 5 and 6; and (4) Eppler, by R. Eppler and D. Somers and soon to be documented in a NASA Technical Note. It should be mentioned that the versions of these computer codes in use at GA/ADAC are maintained as up-to-date as possible; yet, in some instances, these versions are not the most current since each of the codes, with the exception of the Smetana code, is constantly being refined and improved by the respective program authors. For example, the Carlson code is currently being modified to include the effects of a laminar boundary layer and the Eppler code may soon be modified to iterate on the boundary layer displacement thickness.

A brief description of the method of approach for the four codes will be given here; the literature cited (refs. 1-6) contains the detailed explanations. The Garabedian code is a transonic code that employs a finite difference solution to the full inviscid potential flow equation for a conformally mapped airfoil. The boundary layer displacement is added iteratively to the airfoil ordinates in order to evaluate airfoil section performance including viscous effects. The Carlson code is also a transonic code and is similar to Garabedian, but it uses a finite difference solution to the full inviscid potential flow equation for an airfoil in a stretched Cartesian coordinate system, instead of for a conformally mapped airfoil. The Smetana program is a strictly subcritical code employing a method of vorticity distributed over an airfoil approximated by a closed polygon. An iterative approach to boundary layer effects is included. The approach used in the Eppler code is similar to the Smetana code, but it differs in that the vorticity is distributed over an airfoil shape approximated by curved panels and that there is no iteration on the boundary layer displacement thickness.

A summary of the methods of approach for the inviscid flow and the technique of handling the boundary layer for each computer code is given in table 1. The iterative procedure referred to in table 1 is that of: (1) obtaining an inviscid flow solution for the original airfoil; (2) obtaining a boundary layer solution based on the inviscid flow solution; (3) modifying the airfoil shape by adding the boundary layer displacement thickness to the airfoil; (4) obtaining an inviscid flow solution for the modified airfoil; and, (5) repeating steps 2 through 4 until convergence criteria are satisfied.

AIRFOIL SECTIONS

Three classes of airfoil section geometries are included in these comparative results. A symmetrical airfoil section is represented by the well documented NACA 0012 profile (ref. 7 and 8) shown in figure 1. To provide a sufficient number of airfoil ordinates for computational purposes, computer generated coordinates for the NACA 0012 (ref. 9) were used with the airfoil section being defined by 47 ordinates for both upper and lower surfaces. Although no attempt has been made in this work to evaluate the performance of the individual computer codes with respect to sensitivity of computational results to airfoil ordinate density, a sufficient number of coordinates (i.e. at least 35 to 40) has been used to provide consistent, reliable results. Ordinate density has been distributed such that there is a higher density of points concentrated in regions of greater airfoil curvature. This is a particular requirement for the two subcritical codes because of the nature of the distributed vorticity methods of flow solution.

Results for a conventional section are illustrated by a NACA 65A413 airfoil (fig. 2). The ordinates for this section, 63 in number, were obtained by the method of reference 10. Some drag prediction comparisons for another NACA 6A-series section, a 64A010, are also included.

The third class of airfoil geometries investigated is the aft-cambered Whitcomb supercritical type section. In this paper, the results for a derivative of such a section designed specifically for general aviation applications, the NASA LS(1)-0413 airfoil (fig. 3), are presented. The ordinates used for the LS(1)-0413, known also as the GA(W)-2 airfoil, are those listed in reference 11.

AIRFOIL DATA SUMMARY COMPARISONS

For the two subcritical codes, Smetana and Eppler, a comparison of the three airfoils in terms of airfoil data summary plots is of interest. As shown in figure 4 for the NACA 0012, the comparison with experiments reported in reference 7 is quite good. Note that the wind tunnel test is shown as the solid line while the theory is given by the symbols, a reversal of usual conventions. The Eppler code shows a break-over in the C_L (lift coefficient)

versus alpha (angle of attack) plot produced by using the predicted separation point to define an "effective" angle of attack. The Smetana code merely identifies a predicted separation point, but makes no attempt to compensate for the effects of separation. The free transition option was specified in the Smetana code for this comparison and the following two airfoil data summaries. The Eppler code always uses natural transition, although it does allow a variable roughness option.

In figure 5, computational results are shown for a NACA 65A413 airfoil compared to the wind tunnel results for a NACA 65_1-412 of reference 7. Both codes may be observed to predict the laminar drag bucket for this NACA 6-series section.

The airfoil data summary comparisons for the NASA LS(1)-0413, shown in figure 6, point out the difficulty Eppler has with some airfoils with regard to the angle of zero lift. This appears to be related to the lack of an iterative boundary layer solution and is more noticeable with supercritical type, blunt trailing edged airfoil shapes. The wind tunnel results are those of McGhee, et al. (ref. 12).

PRESSURE DISTRIBUTION COMPARISONS

The detailed pressure distribution comparison cases which follow include operating conditions at subcritical and near critical or supercritical Mach numbers. The computational results are compared with experimental results from The Ohio State University 15 cm (6 in.) by 56 cm (22 in.) Transonic Airfoil Tunnel. The OSU 6 x 22 wind tunnel is a low-interference transonic facility for airfoil testing over the Mach number range of 0.30 to 1.07 and a Reynolds number range of 2 to 15 million based on 15.24 cm (6 in.) model chord (refs. 13 and 14). The angle of attack used in the computational results is the effective angle of attack, α_{eff}, obtained from the set angle of attack in the wind tunnel corrected for wall effects according to the empirically derived relation:

$$\alpha_{eff} = \alpha_{set} - 0.17\, C_L$$

It should be noted that for all the supercritical pressure distribution comparisons, the drag coefficient listed for Carlson has been omitted. Total drag as predicted by Carlson requires a wave drag correction to be applied that was not available to the authors at this writing.

Figure 7 shows the comparisons for all the codes for the NACA 0012 airfoil at a Mach number of about 0.35 over a range of angles of attack. The pressure distributions are in good agreement, though the Eppler code predicts a somewhat higher suction peak than the other codes at the higher angles of attack. Drag comparisons for the subcritical codes using the free transition option are quite good. The less accurate drag predictions by the two transonic codes is a result of attempting to simulate free transition by fixing turbulent boundary

layer transition a few percent chord in front of the Smetana predicted naturally occurring transition location.

Comparisons for the NACA 0012 at an angle of attack of zero over a range of Mach numbers is given in figure 8. Both the Smetana and Eppler codes show a tendency to predict lower pressures in the nose region at the near critical Mach number condition, and of course can not correctly predict the distribution at supercritical conditions. Both transonic codes identify the strength and location of the shock quite well.

Comparisons of the transonic codes and wind tunnel results for the NACA 0012 at supercritical conditions are given in figure 9. The Mach number is nominally 0.80 and results are given for three angles of attack. Note that the Carlson code appears to predict somewhat higher values of lift and a corresponding prediction of a shock located further aft on the airfoil. This appears to be caused by an uncertainty in angle of attack in the Carlson code, with a trend toward results being obtained at a slightly higher angle of attack than the input angle of attack for many airfoils. Thus, in general. Carlson results should be examined as pressure versus lift coefficient, moment versus lift coefficient, etc., instead of angle of attack. Since direct comparisons with wind tunnel angle of attack were desired for this study, matching angle of attack was more convenient, so this approach has been used. Both codes indicate a tendency to recover more pressure on the aft upper surface than is observed in the wind tunnel tests for this airfoil (and most other airfoils as well). In figure 9c the large discrepancy in shock location may be explained by the fact that the predicted local Mach number in front of the shock is in excess of 1.47, a shock Mach number that poses difficulty for both the theory and the wind tunnel.

For the transonic codes, careful selection of input parameters relating to convergence and relaxation factors are required to encourage the codes to produce any meaningful results for an airfoil when the free stream Mach number and lift coefficient exceed certain values. The empirical relationship below, suggested by Dr. R. Whitcomb, appears to describe these limiting values:

$$M + t/c + 0.1\, C_L \geq 0.92$$

Here M is the free stream Mach number, t/c is the airfoil thickness ratio and C_L is the lift coefficient.

In figures 10 and 11, results are presented for the NACA 65A413 airfoil section for a subcritical and slightly supercritical Mach number. This comparison shows both the Garabedian and Carlson codes over-predicting the lift. Carlson's over-prediction could be related to the angle of attack uncertainty previously discussed but no consistent reason can be presented for Garabedian's results, particularly for the generally higher pressures predicted on the lower surface (fig. 10). This characteristic in Garabedian occurs infrequently and may be circumvented by using the matching-lift-coefficient option (which essentially compensates for any uncertainty in angle of attack in either the wind tunnel or computer code). Also, the theoretical predictions of drag, though consistent with each other, are lower than the wind tunnel results.

(The wave drag contribution in figure 11 is less than 0.0002, and thus the Carlson skin friction drag as shown approximates the total drag).

Comparisons for the NASA LS(1)-0413 airfoil section are given in figures 12 and 13. Figure 12 shows the computational and experimental results obtained for a nearly zero angle of attack through a range of Mach numbers from 0.45 to 0.80. For this airfoil, agreement with the wind tunnel results at subcritical conditions is excellent for both the pressure distributions and the aerodynamic coefficients. It is interesting to note in figure 12c that the pressure distributions and shock locations predicted by Garabedian and Carlson differ noticeably, presumably for reasons mentioned earlier; yet in figure 12d the pressure distributions predicted by the codes are nearly identical. (The wind tunnel results in 12d may be influenced by the strong shock present at the condition illustrated). This comparison points out the uncertainties in angle of attack are dependent not only on the input airfoil but also on the specific input conditions as well.

The results for the NASA LS(1)-0413 at a nominal Mach number of 0.72 over a range of angles of attack are presented in figure 13. In figure 13a, both transonic codes exhibit some interesting characteristics. Carlson, although the lift nearly matches the wind tunnel results, has difficulty properly defining the nose region on the lower surface. This may be due to the fact the Cartesian grid used does not place a large number of computational points near the leading (and trailing) edge. Although the Garabedian result accurately describes the lower surface nose region including the shock location, the lift prediction is too low as a result of over-predicting the pressure recovery on the upper surface. In figure 13b these same trends may be observed to a lesser degree. In 13c the results are more characteristic of the codes: Garabedian showing a reasonable lift and drag prediction with a slightly higher than wind tunnel observed pressure recovery over the trailing edge region; and Carlson exhibiting results at an apparently higher effective angle of attack for the input angle of attack which matches the wind tunnel and the Garabedian results.

In figure 14, comparisons are shown for Carlson with wind tunnel results (fig. 13c) by both matching angle of attack and selecting angle of attack which is matching the wind tunnel lift coefficient. Note that the expected excellent agreement of the pressure distribution and the aerodynamic coefficients with the wind tunnel test is obtained when lift coefficients are matched.

DRAG PREDICTIONS

Drag coefficient predictions by the Garabedian code are generally consistent and accurate enough to enable use of the code to predict the drag rise characteristics and the drag divergence Mach number for most airfoils. The version of the Garabedian code in use at GA/ADAC for the past 18 months employs the latest wave drag calculation techniques and the fast Poisson solver for the subsonic region of flow which improves the rate of convergence (ref. 2).

Figure 15 shows good agreement between the Garabedian code predicted and the OSU 6 by 22 wind tunnel observed total drag for Mach numbers well into the drag rise. It should be noted that the Reynolds number was not to be held constant in these results, but varied from 3.8 to 5.9 million. The angle of attack was nominally zero. Transition was specified as fixed at 0.075c for the Garabedian code which seems consistent for the LS(1)-0413, a turbulent flow airfoil by design, at these conditions. The sudden decrease in skin friction drag shown for this airfoil in the drag rise region is a result of shock-induced separation due to the strong shock present. The relatively larger region of computer predicted separated flow behind the shock on the upper surface of the airfoil results in a lower skin friction drag coefficient.

Drag rise characteristics for the symmetric, NACA 64A010 airfoil section are given in figure 16. Excellent agreement between theory and wind tunnel is again observed. The boundary layer transition was fixed at 0.05c in both the wind tunnel and computer code. The Reynolds number varied from 3.5 million at Mach 0.5 to about 5 million at Mach 0.85. The angle of attack was held at zero.

COMPUTER REQUIREMENTS

All four airfoil analysis codes are run on the GA/ADAC computer facility located at AARL. The computer system is a dual processor system using Harris SLASH 6 and SLASH 5 processors. The SLASH 6, which is used for all of GA/ADAC's airfoil work, is a medium-sized, 24 bit word computer system with 64K words (192K bytes) of main memory. For purposes of comparison, the SLASH 6 is about an average factor of 8 times slower in heavy floating point FORTRAN programs than an IBM System 370 Model 168. Of special interest is the fact the calculations on the SLASH 6 are performed with over 11 decimal digits of accuracy while single precision on IBM mainframes affords approximately 7 decimal digits accuracy. The 11+ digit accuracy of the computer used at GA/ADAC is well suited for most scientific calculations including airfoil analysis, thus avoiding the necessity to maintain 15-16 digit accuracy like that of a CDC mainframe or double precision on an IBM machine.

Table 2 lists several computer related characteristics of the four codes. Of most interest are the memory requirements and the run times for the programs. All the codes have been folded into the SLASH 6 such that the largest program requires 48K words. All programs are overlaid to varying degrees to reduce memory requirements. Per case run times, where a "case" is a calculation at one Mach number, one Reynolds number, and one angle of attack, are expressed in a normalized form. The single case run time used for normalization is that of the Smetana code. For the SLASH 6, time T is on the order of 90-100 seconds. A range of times is shown for the two transonic codes since convergence to a solution varies depending on whether the case is subcritical or supercritical and on a user-supplied convergence tolerance. The Carlson code has the longest running time per case when results are carried to the fine grid, which was used in all cases for the previous comparisons. The medium grid result of

Carlson can be used if desired with an accompanying reduction in computation time. The Smetana code has no convergence criteria, relying instead on a program-fixed number of inviscid flow/boundary layer iterations to achieve a converged solution and resulting in a very consistent run time per case. The Eppler code is the most rapid of the four codes and typically requires a small percentage of time T per case. All of the codes have some form of hard copy plot capability.

OBSERVATIONS AND CONCLUSIONS

Based on the results presented here and the extensive exercise of these four single-element airfoil analysis codes, the following observations and remarks can be made.

THE SMETANA CODE: is a subcritical code; uses vorticity distributed around a closed polygonal airfoil; is reasonably well documented; has flexible boundary layer routines, allowing free or fixed transition; has had drag prediction "tuned" for flight Reynolds numbers, giving good drag coefficients over the Reynolds number range of 1 to 15 million; obtains the pressure distribution from iteration with boundary layer; exhibits good angle of zero lift identification; and identifies laminar bubbles. But it: has no design mode; incorporates no evaluation of the effects of boundary layer separation; has a convergence criteria no more sophisticated than a fixed number of iterations; and may provide misleading drag results at low Reynolds numbers due to the tuning factor applied to the drag calculations.

THE EPPLER CODE: is a subcritical code; uses vorticity distributed around a curved panel airfoil; has good boundary layer routines, applicable over a wide range of Reynolds numbers; exhibits good performance at low Reynolds numbers; has a design mode, although the mode is difficult to use at first; provides a separation effects estimate, giving rise to a predicted break in lift coefficient versus angle of attack; executes very quickly, resulting in inexpensive per case computing costs; and contains more empiricism than the other codes. But it: has no iteration with the boundary layer; exhibits difficulty in identifying angle of zero lift, especially for airfoils of the supercritical type cusped trailing edge (which is related to no boundary layer iteration); and has limited documentation.

THE GARABEDIAN CODE: is a transonic code; employs a finite difference solution to the full inviscid potential flow equation for a conformally mapped airfoil; iterates on boundary layer displacement thickness; gives good pressure distributions and shock location as long as the local Mach number does not exceed 1.4; provides reasonable wave drag estimates and can be used for drag rise predictions; and has flexible input options, allowing to specify either angle of attack or coefficient of lift. But it: has no laminar boundary layer or transition criteria; employs a boundary layer smoothing process which can tend to artifically thicken the boundary layer and slow down convergence; and is not well suited for Mach numbers less than 0.3.

THE CARLSON CODE: is a transonic code; employs a finite difference solution to the full inviscid potential flow equation for an airfoil in a stretched Cartesian coordinate system; iterates on boundary layer thickness; gives good pressure distributions; has easy to use design mode; and incorporates a massive separation prediction technique. But it: has no laminar boundary or transition criteria (but one is currently being added); does not have an input option for matching lift coefficient; exhibits an uncertainty in angle of attack; and needs improvement in prediction of the wave drag coefficient.

APPENDIX

SYMBOLS

Measurements and calculations were made in the U.S. Customary Units. They are presented herein in the International System of Units (SI) with the equivalent values given parenthetically in the U.S. Customary Units.

α	angle of attack, deg
c	chord
C_D	drag coefficient
C_L	lift coefficient
C_M	pitching-moment coefficient
C_P	pressure coefficient
K	= 1024
M	Mach number
RE	Reynolds number
T	computer solution time per case
t/c	airfoil thickness-to-chord ratio

REFERENCES

1. Bauer, F., Garabedian, P., Korn, D., and Jameson, A., Supercritical Wing Sections II, A Handbook, Lecture Notes in Economics and Mathematical Systems, Vol. 108, Springer-Verlag, New York, 1975.

2. Bauer, F., Garabedian, P., and Korn, D., Supercritical Wing Sections III, Lecture Notes in Economics and Mathematical Systems, Vol. 150, Springer-Verlag, New York, 1977.

3. Carlson, L. A., "Transonic Airfoil Analysis and Design Using Cartesian Coordinates", Journal of Aircraft, Vol. 13, No. 5, May 1976, pp. 349-356.

4. Carlson, L. A., "TRANDES: A FORTRAN Program for Transonic Airfoil Analysis or Design", NASA CR-2821, June 1977.

5. Smetana, F. O., Summey, D. C., Smith, N. S., and Carden, R. K., "Light Aircraft Lift, Drag, and Moment Prediction - A Review and Analysis", NASA CR-2523, May 1975.

6. Stevens, W. A., Goradia, S. H., and Braden, J. A., "Mathematical Model For Two-Dimensional Multi-Component Airfoils in Viscous Flows", NASA CR-1843, July 1971.

7. Abbott, Ira H., von Doenhoff, Albert E., Theory of Wing Sections, Including A Summary of Airfoil Data, Dover Publications, Inc., New York, 1959.

8. Abbott, Ira H., von Doenhoff, Albert E., and Stivers, Louis S., "Summary of Airfoil Data", NACA TR 824, 1945.

9. Ladson, C. L., and Brooks, C. W., "Development of a Computer Program to Obtain Ordinates for NACA 4-Digit, 4-Digit Modified, 5-Digit, and 16 Series Airfoils", NASA TM X-3284, November 1975.

10. Ladson, C. L., and Brooks, C. W., "Development of a Computer Program to Obtain Ordinates for NACA 6- and 6A-Series Airfoils", NASA TM X-3069, September 1974.

11. McGhee, Robert J., and Beasley, William D., "Effects of Thickness of an Initial Low-Speed Family of Airfoils for General Aviation Applications", NASA TM X-72843, June 1976.

12. McGhee, Robert J., Beasley, William D., and Somers, Dan W., "Low-Speed Aerodynamic Characteristics of a 13-Percent-Thick Airfoil Section Designed for General Aviation Applications", NASA TM X-72697, 1975.

13. Lee, John D., "Evaluation of Interference in the OSU 6 in. by 22 in. Transonic Airfoil Tunnel", Advanced Technology Airfoil Research, Volume I, NASA CP-2045, Pt. 2, 1979. (Paper 34 of this compilation.)

14. Lee, John D., Gregorek, G. M., and Korkan, K. D., "Testing Techniques and Interference Evaluation in the OSU Transonic Airfoil Facility", AIAA Paper No. 78-1118, presented at the 11th AIAA Fluid and Plasma Dynamics Conference, Seattle, Washington, July 10-12, 1978.

TABLE 1. COMPARISON OF FOUR SINGLE ELEMENT AIRFOIL ANALYSIS CODES

COMPUTER CODE	SOLUTION APPROACH	BOUNDARY LAYER CHARACTERISTICS			
		ITERATIVE	LAMINAR	TRANSITION	TURBULENT
Garabedian, et al.	Transonic, finite difference solution of full inviscid potential flow equation for conformally mapped airfoil	Yes	No	Fixed only	Nash-Macdonald
Carlson	Transonic, finite difference solution of full inviscid potential flow equation for airfoil in stretched Cartesian coordinates	Yes	No	Fixed only	Nash-Macdonald
Smetana, et al.	Subcritical, distributed vorticity over an airfoil shape approximated by a closed polygon	Yes	Yes	Natural or fixed	Goradia, and Truckenbrodt
Eppler	Subcritical, distributed vorticity over an airfoil shape approximated by curved panels	No	Yes	Natural only, variable "roughness"	Empirical

TABLE 2. COMPUTER RELATED CHARACTERISTICS OF FOUR SINGLE ELEMENT AIRFOIL ANALYSIS CODES.

COMPUTER CODE	DESIGN MODE	MEMORY* REQUIREMENTS	HARD COPY PLOT CAPABILITY	SOURCE STATEMENTS	PER CASE RUN TIMES
Garabedian, et al.	No**	48,000	Yes	3080	10T-20T
Carlson	Yes	43,000	Printer Plot	2586	10T-36T
Smetana, et al.	No	28,000	Yes	2458	T***
Eppler	Yes	43,000	Yes	2050	0.15T

*All programs are overlaid on GA/ADAC Computer System, requirements listed in words.

**A separate design code by Garabedian, et al., is available (ref. 2).

***Time T is approximately 90-100 seconds on GA/ADAC computer system.

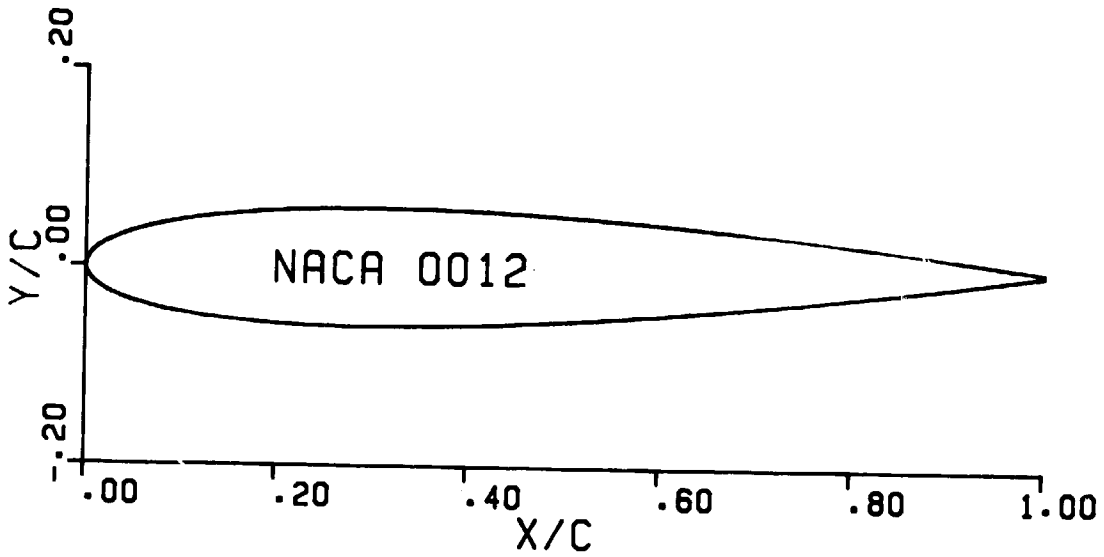

Figure 1.- The NACA 0012 airfoil section.

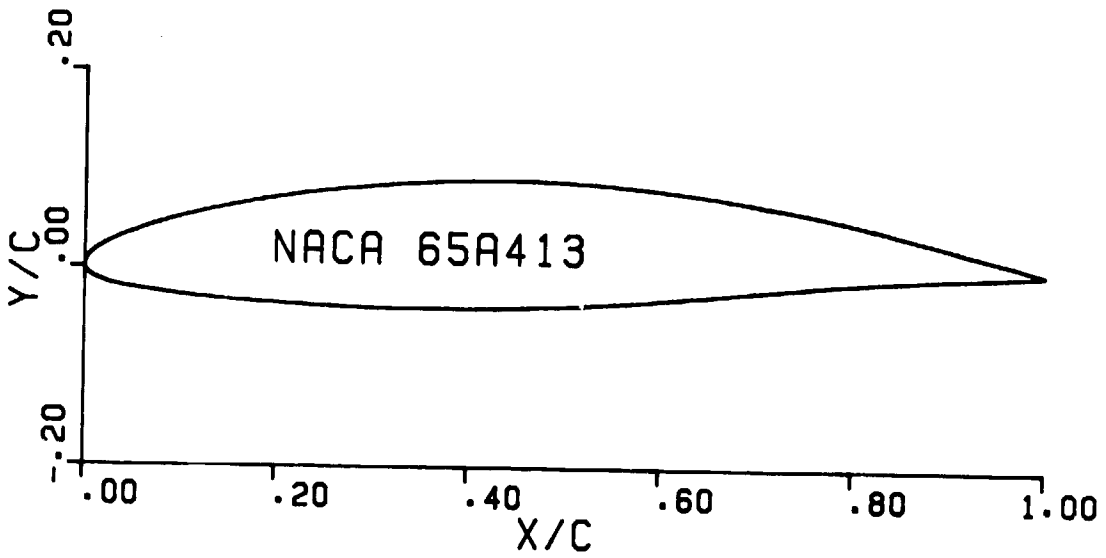

Figure 2.- The NACA 65A413 airfoil section.

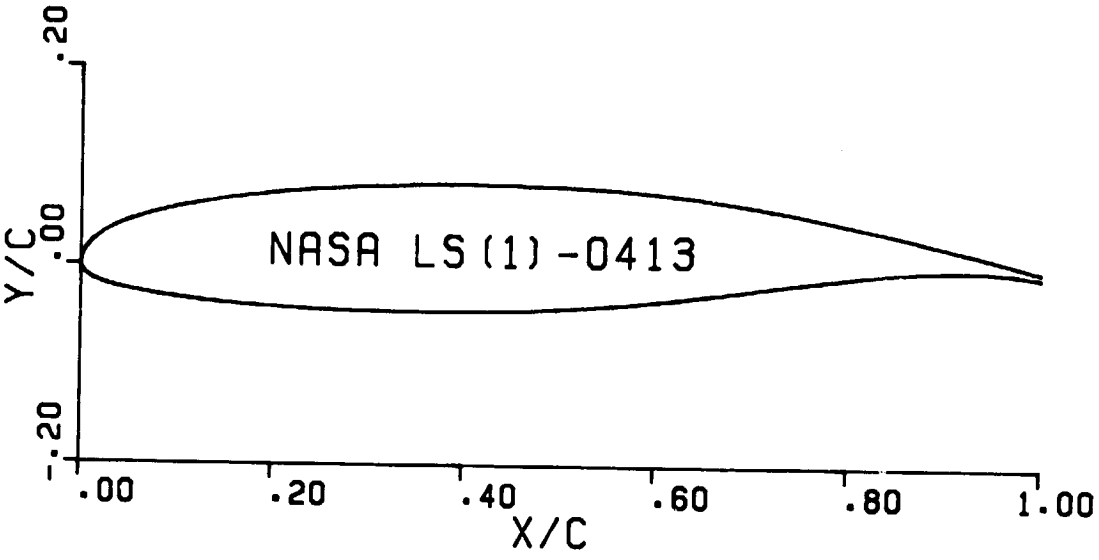

Figure 3.- The NASA LS(1)-0413 airfoil section.

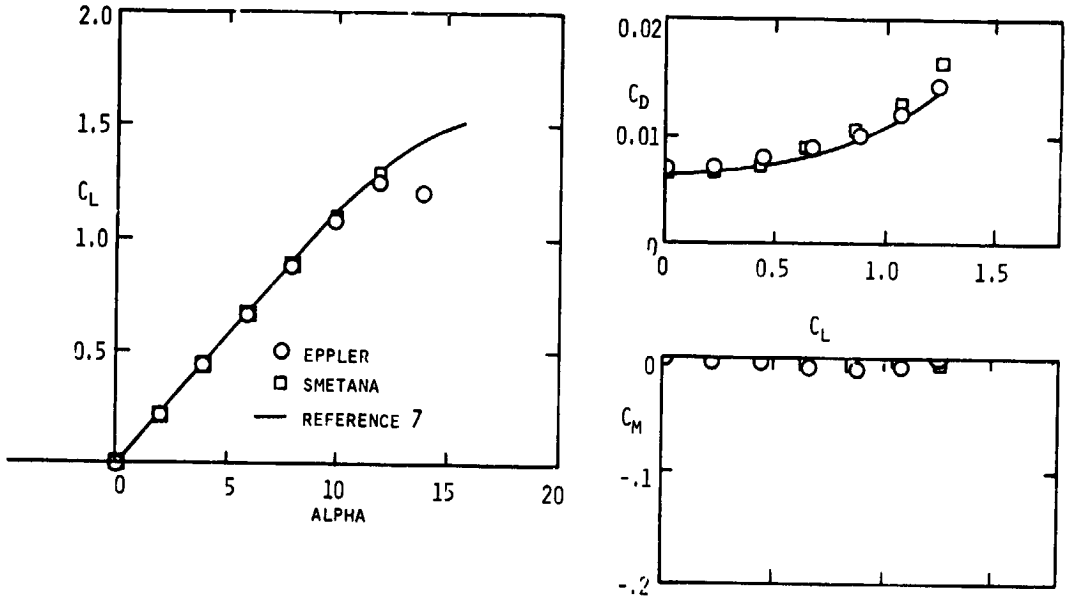

Figure 4.- NACA 0012 airfoil-section characteristics. Computational results are for a Reynolds number of 6 million at a Mach number of 0.20.

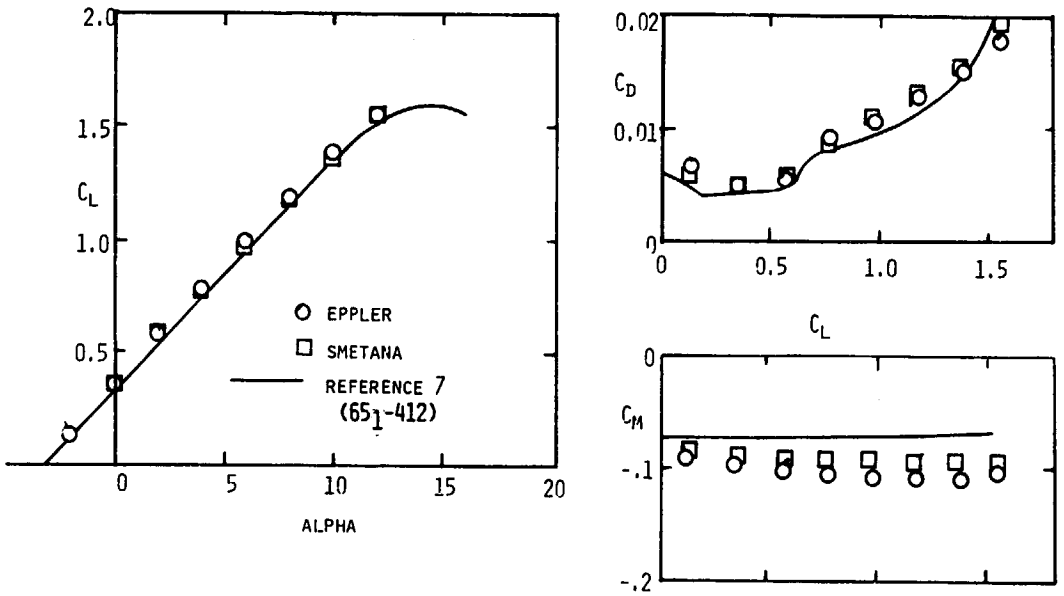

Figure 5.- NACA 65A413 airfoil-section characteristics. Computational results are for a Reynolds number of 6 million at a Mach number of 0.20. Comparison is made to a 65_1-412 airfoil of reference 7.

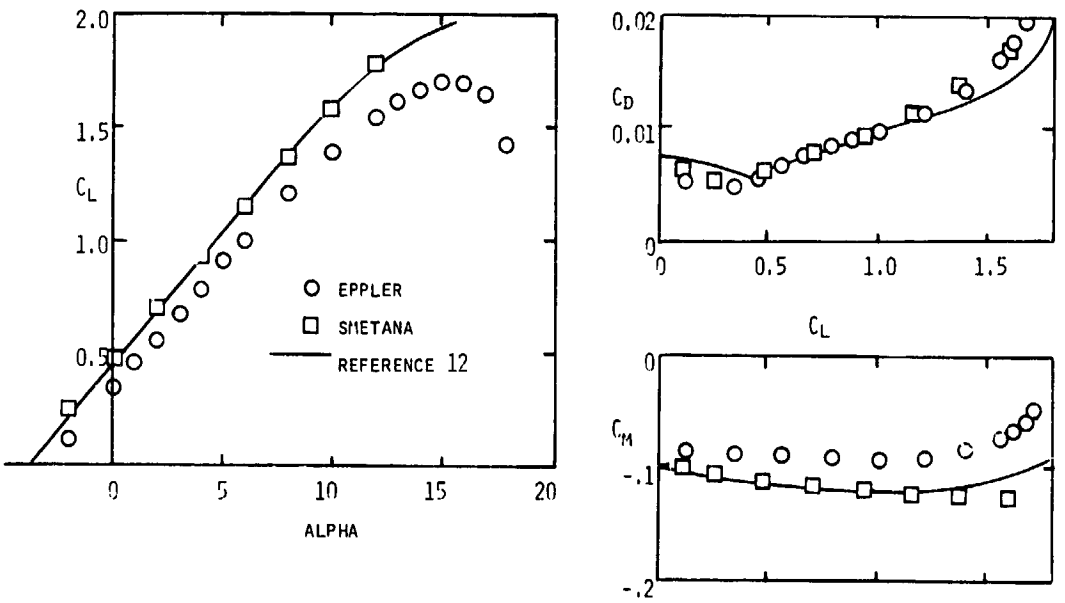

Figure 6.- NASA LS(1)-0413 airfoil-section characteristics. Computational results are for a Reynolds number of 6 million at a Mach number of 0.20.

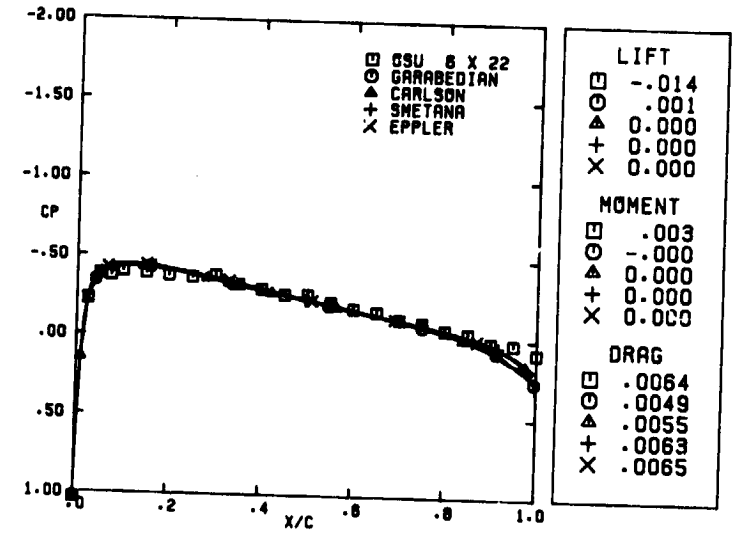

(a) M = 0.351; RE = 3.65 million; $\alpha = 0^{\circ}$.

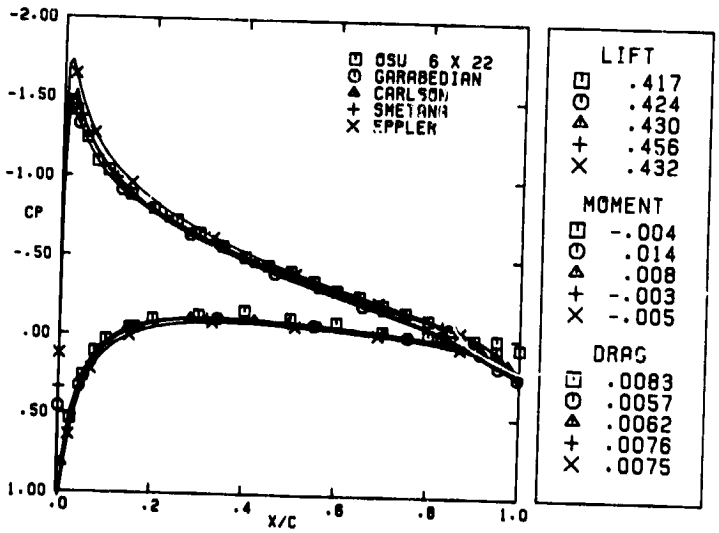

(b) M = 0.345; RE = 3.24 million; $\alpha = 3.93^{\circ}$.

Figure 7.- Comparison of computer-code predictions with wind-tunnel results for an NACA 0012 airfoil section at a subcritical Mach number over a range of angles of attack.

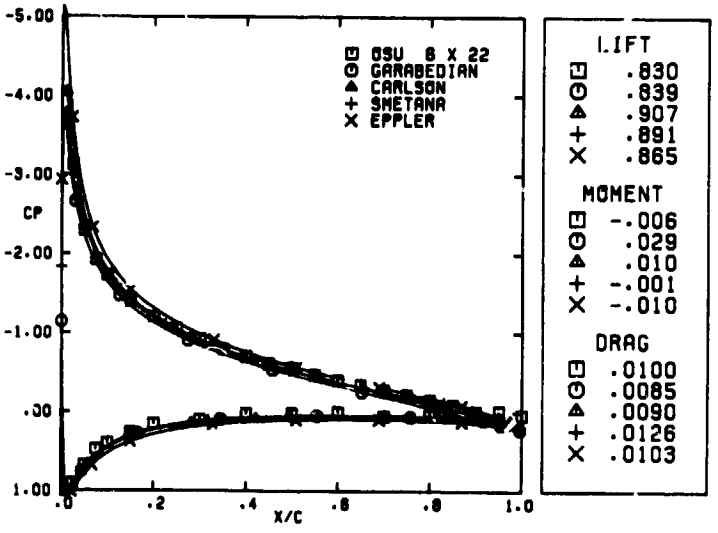

(c) M = 0.342; RE = 3.39 million; $\alpha = 7.88^{o}$.

Figure 7.- Concluded.

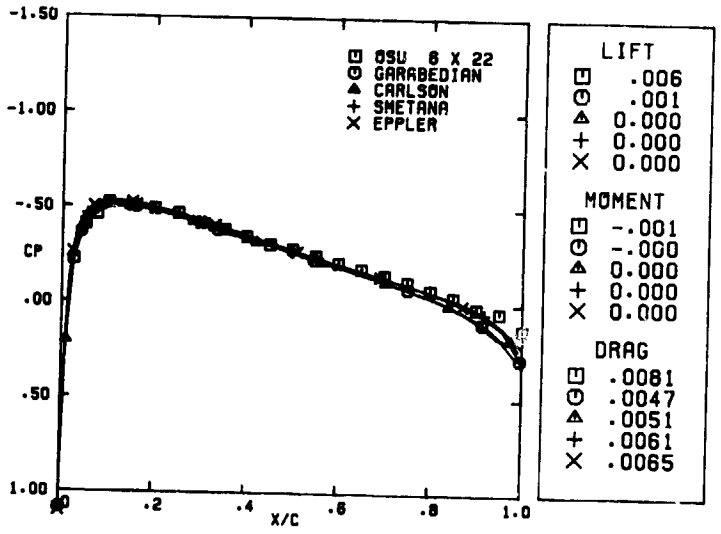

(a) M = 0.575; RE = 4.68 million.

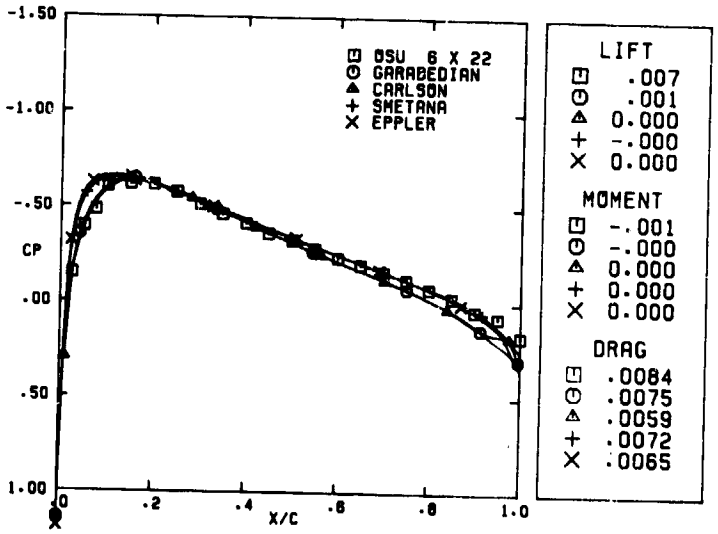

(b) M = 0.725; RE = 5.34 million.

Figure 8.- Comparison of computer-code predictions with wind-tunnel results for an NACA 0012 airfoil section at an angle of attack of zero over a range of Mach numbers.

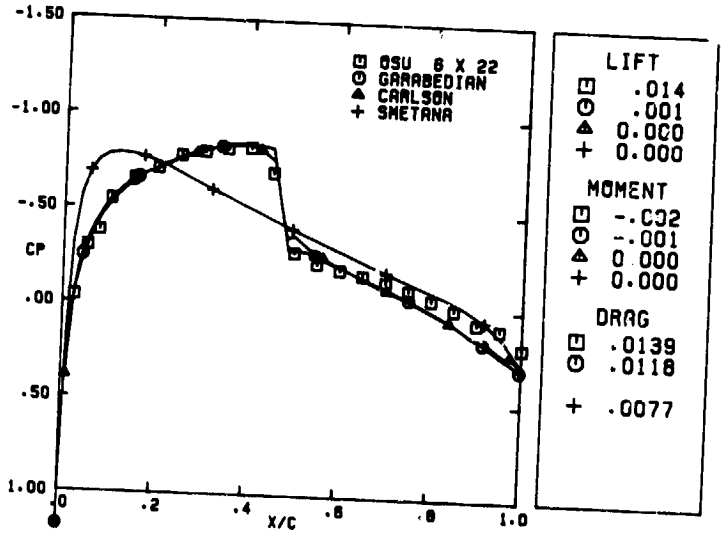

(c) M = 0.808; RE = 6.12 million.

Figure 8.- Concluded.

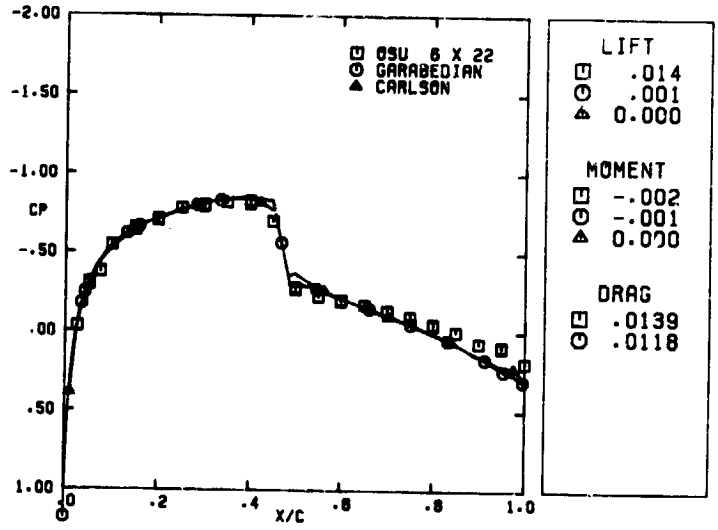

(a) M = 0.808; RE = 6.12 million; $\alpha = 0^{\circ}$.

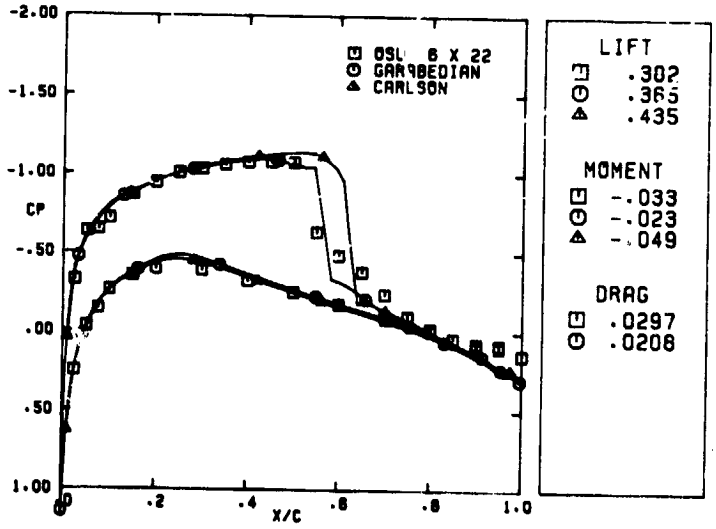

(b) M = 0.804; RE = 5.57 million; $\alpha = 1.94^{\circ}$.

Figure 9.- Comparison of computer-code predictions with wind-tunnel results for an NACA 0012 airfoil section at a supercritical Mach number over a range of angles of attack.

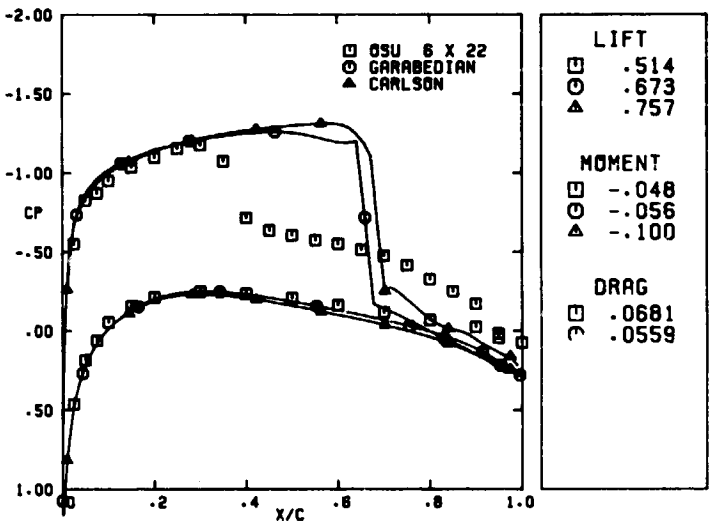

(c) M = 0.803; RE = 6.31 million; $\alpha = 3.92^{\circ}$.

Figure 9.- Concluded.

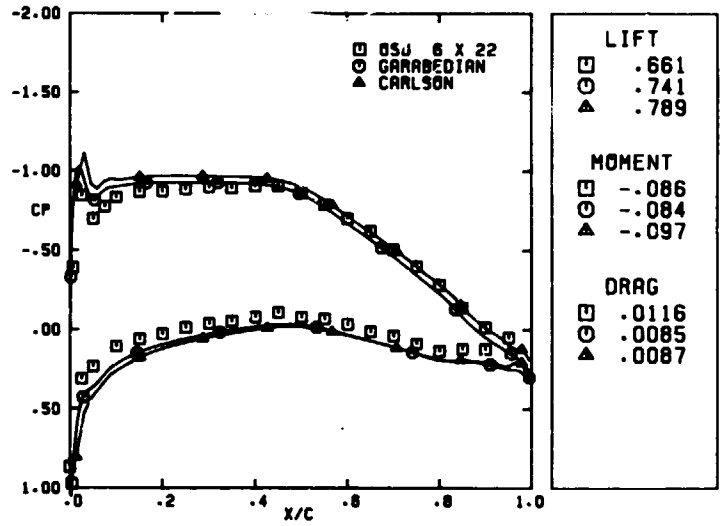

Figure 10.- Comparison of computer-code predictions with wind-tunnel results for an NACA 65A413 airfoil section at M = 0.517, RE = 7.08 million, and $\alpha = 2.90^{\circ}$.

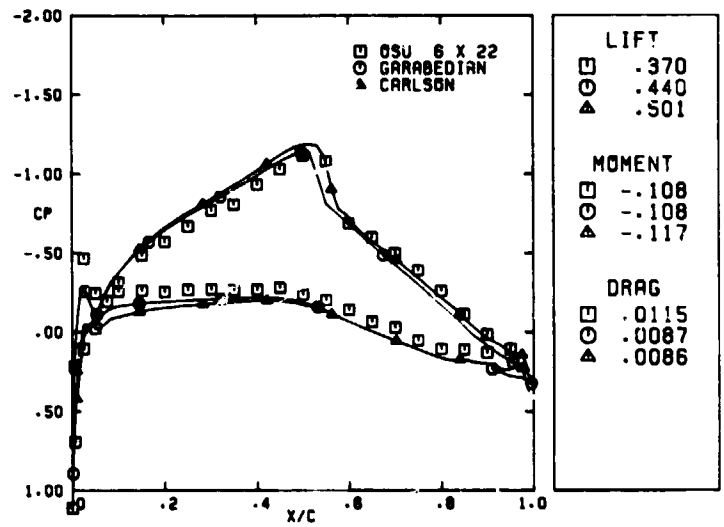

Figure 11.- Comparison of computer-code predictions with wind-tunnel results for an NACA 65A413 airfoil section at M = 0.700, RE = 8.20 million, and $\alpha = -0.06^{\circ}$.

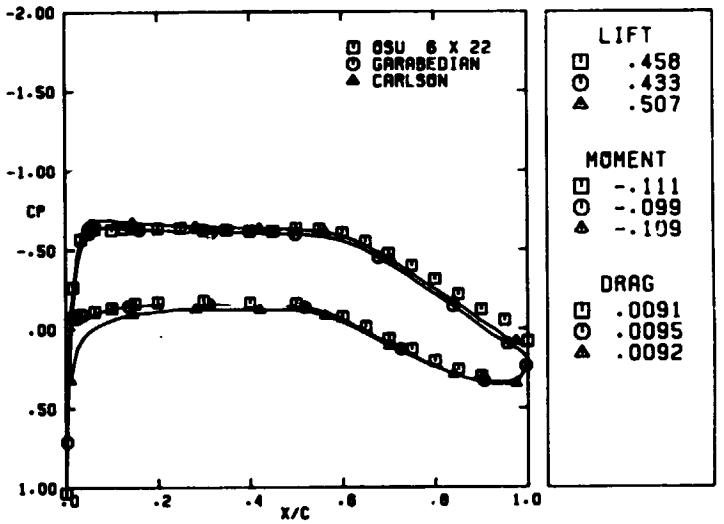

(a) M = 0.454; RE = 3.75 million; $\alpha = -0.07^{\circ}$.

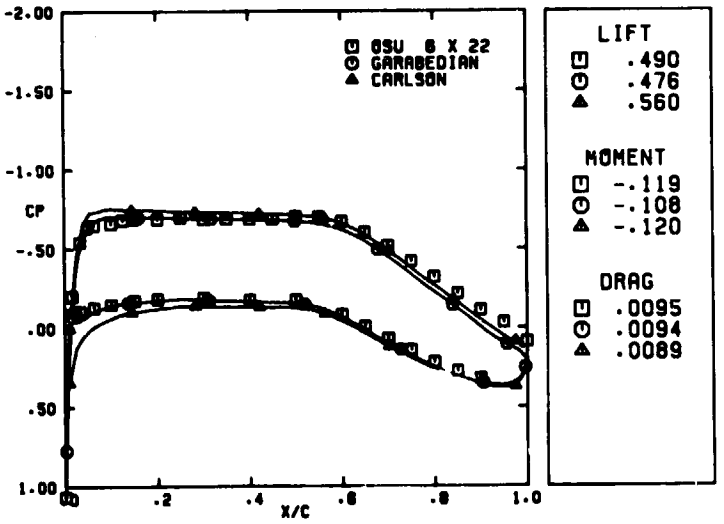

(b) M = 0.578; RE = 4.98 million; $\alpha = -0.07^{\circ}$.

Figure 12.- Comparison of computer-code predictions with wind-tunnel results for an NASA LS(1)-0413 airfoil section at an angle of attack of zero over a range of Mach numbers.

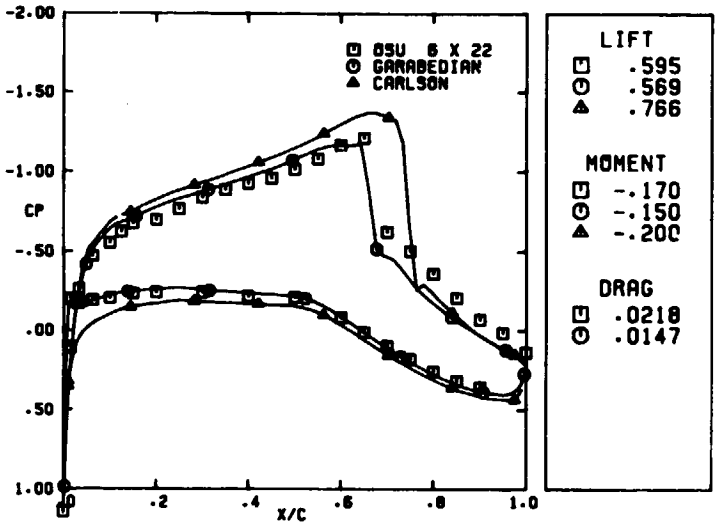

(c) M = 0.755; RE = 5.11 million; $\alpha = -0.06^{\circ}$.

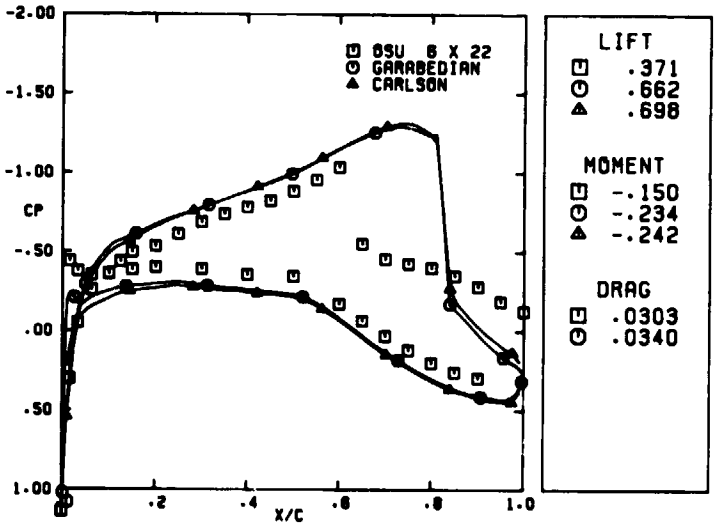

(d) M = 0.802; RE = 5.90 million; $\alpha = -0.06^{\circ}$.

Figure 12.- Concluded.

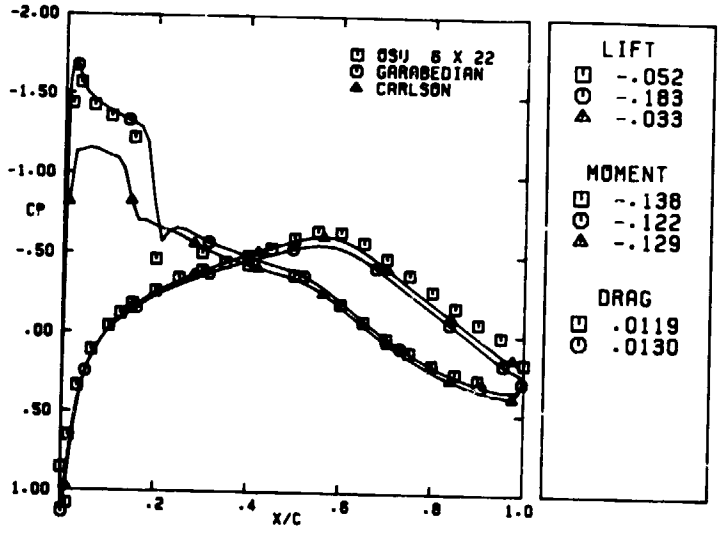

(a) M = 0.722; RE = 4.68 million; $\alpha = -3.99^{\circ}$.

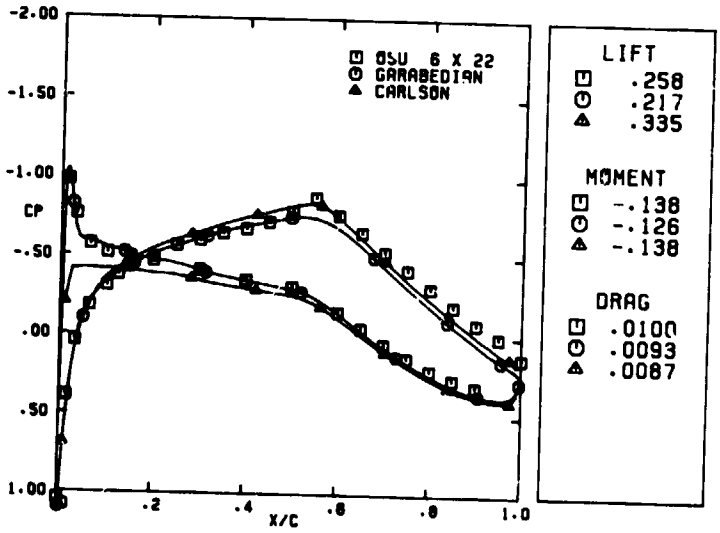

(b) M = 0.721; RE = 6.03 million; $\alpha = -2.04^{\circ}$.

Figure 13.- Comparison of computer-code predictions with wind-tunnel results for an NASA LS(1)-0413 airfoil section at a Mach number of 0.722 over a range of angles of attack.

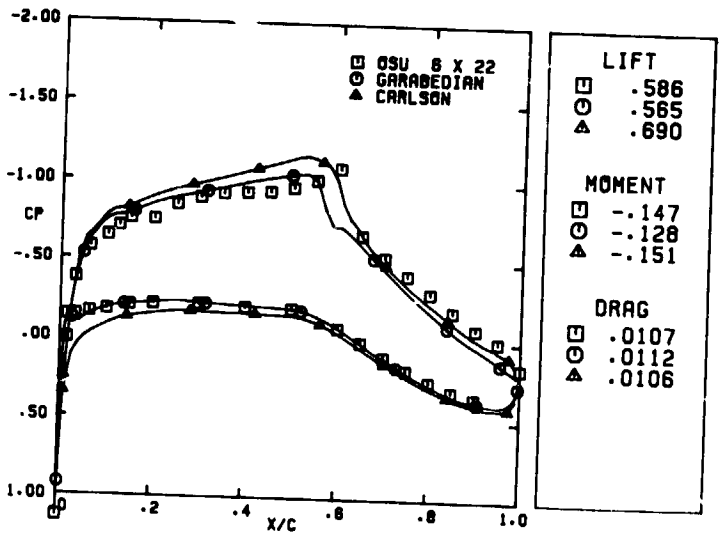

(c) M = 0.722; RE = 4.69 million; $\alpha = -0.09^c$

Figure 13.- Concluded.

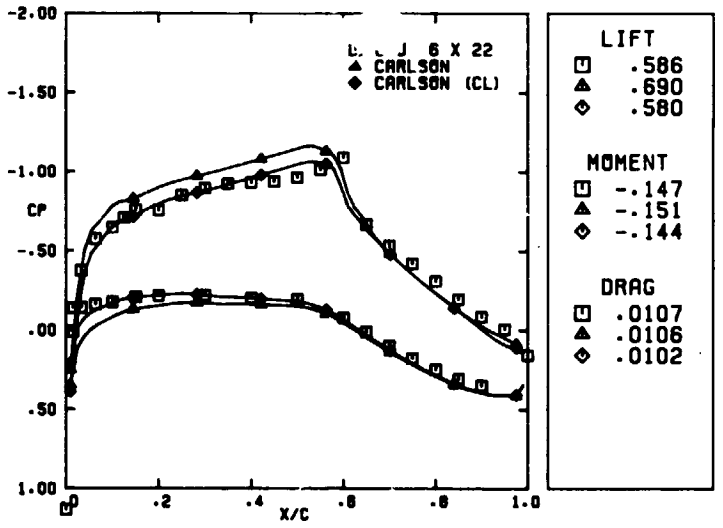

Figure 14.- Comparison of results from the Carlson code obtained by attempting to match lift coefficient to wind-tunnel result. NASA LS(1)-0413 airfoil; M = 0.722; RE = 4.69 million; $\alpha = -0.09^{o}$.

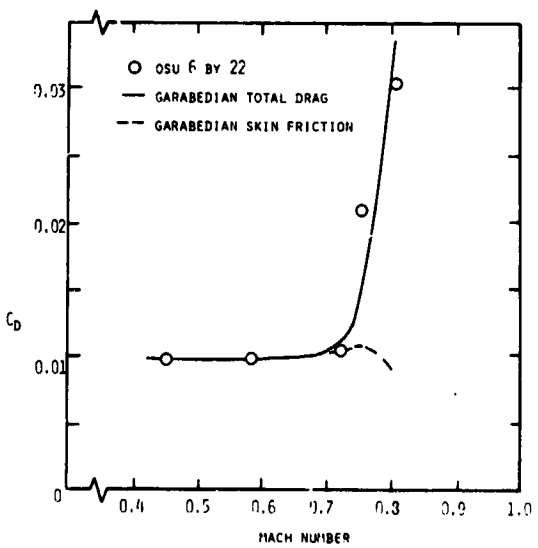

Figure 15.- Comparison of the Garabedian code prediction and wind-tunnel result for the drag-divergence characteristics of the NASA LS(1)-0413 airfoil section at zero angle of attack.

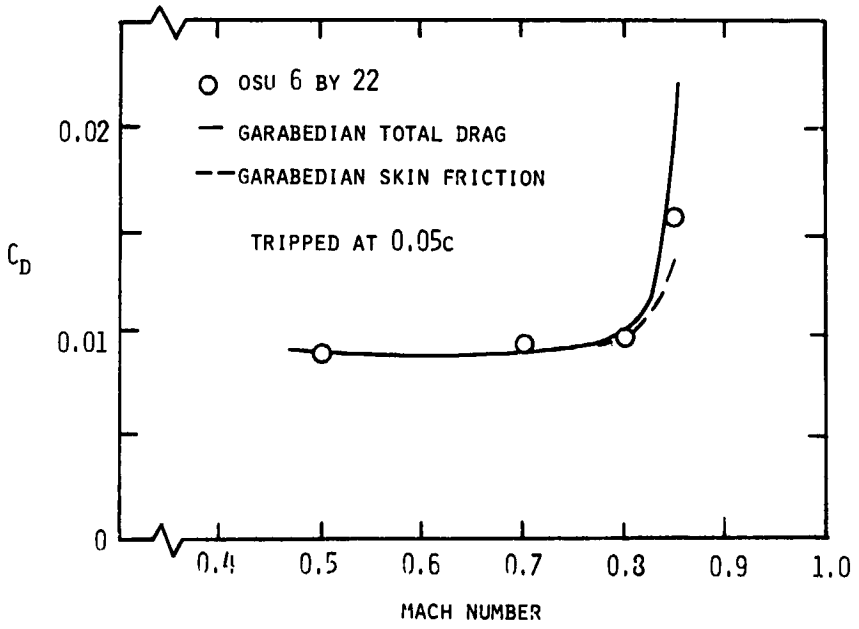

Figure 16.- Comparison of the Garabedian code prediction and wind-tunnel result for the drag-divergence characteristics of the NACA 64A010 airfoil section at zero angle of attack.